Br. J. Pharmacol. (1994), **111**, 598–608

Calcium-dependence of histamine- and carbachol-induced inositol phosphate formation in human U373 MG astrocytoma cells: comparison with HeLa cells and brain slices

J.A. Arias-Montaño, V. Berger & [1]J.M. Young

Department of Pharmacology, University of Cambridge, Tennis Court Road, Cambridge CB2 1QJ

1 Histamine (1 mM) induced an accumulation of inositol monophosphate ([^{3}H]-IP_1) in the U373 MG human astrocytoma cell line which increased with time in the presence of 30 mM Li^+. After a 30 min incubation period with 1 mM histamine [^{3}H]-IP_1 was the major product detected (84 ± 1% of total [^{3}H]-IP_x) and was present at a level 11 (± 1) fold of basal accumulation.

2 Concentration-response curves for histamine-induced [^{3}H]-IP_1 accumulation in U373 MG cells (EC_{50} 5.4 ± 0.5 μM) were shifted to the right in a parallel fashion by mepyramine (slope of a Schild plot 0.99 ± 0.08), yielding a K_d for mepyramine of 3.5 ± 0.3 nM, consistent with the involvement of histamine H_1-receptors.

3 The temelastine-sensitive binding of [^{3}H]-mepyramine to a membrane fraction from U373 MG cells was hyperbolic and had a mean K_d of 2.5 ± 1.0 nM. The maximum amount of temelastine-sensitive binding was 86 ± 19 pmol g^{-1} membrane protein.

4 Carbachol also induced [^{3}H]-IP_1 accumulation in U373 MG cells, 2.8 (± 0.1) fold of basal with 1 mM carbachol, with an EC_{50} of 48 ± 8 μM. Pirenzepine shifted carbachol concentration-response curves to the right (slope of Schild plot 0.89 ± 0.07) giving a K_d for pirenzepine of 0.10 ± 0.01 μM, suggesting that phosphoinositide hydrolysis in U373 MG cells is mediated by the M_3-, rather than the M_1-, muscarinic receptor subtype.

5 [^{3}H]-IP_1 accumulation induced by both 1 mM histamine and by 1 mM carbachol increased when the Ca^{2+} concentration of the medium was increased from 'zero' (no added Ca^{2+}) to 0.3 mM. Histamine-stimulated [^{3}H]-IP_1 accumulation was further increased, although not so markedly, as the Ca^{2+} was raised to 4 mM. The same pattern was apparent with histamine-induced accumulations of [^{3}H]-IP_2 and [^{3}H]-IP_3. In contrast, [^{3}H]-IP_x accumulation in response to carbachol increased between 0.3 and 1.3 mM, but thereafter remained unchanged ([^{3}H]-IP_1) or declined ([^{3}H]-IP_2 and [^{3}H]-IP_3).

6 In HeLa cells, [^{3}H]-IP_1 accumulations induced by 1 mM histamine and 1 mM carbachol showed the same pattern of Ca^{2+} dependence and were independent of extracellular Ca^{2+} above 0.3 mM (histamine) or 1.3 mM (carbachol). The response to carbachol appeared to be mediated by an M_3-muscarinic receptor (apparent K_d for pirenzepine 0.09 μM).

7 In cross-chopped slices of guinea-pig cerebral cortex and guinea-pig cerebellum, [^{3}H]-IP_1 accumulation induced by 1 mM histamine in the presence of 10 mM Li^+ increased as the extracellular Ca^{2+} was increased from 0.3 to 2.5 mM, but a further increase to 4 mM had no further effect. In contrast the response to histamine in rat cerebral cortex increased markedly between 1.3 and 4 mM Ca^{2+}. Accumulations of [^{3}H]-IP_1 induced by carbachol in guinea-pig or rat cerebral cortical slices were not increased as extracellular Ca^{2+} was raised from 0.3 to 4 mM.

8 Nimodipine (100 nM) and ω-conotoxin (3 μM) had no significant effect on histamine-induced [^{3}H]-IP_1 accumulation in rat cerebral cortical slices or in U373 MG cells.

9 We conclude that histamine-induced [^{3}H]-IP_1 accumulation in U373 MG cells does appear to have a component dependent on the extracellular Ca^{2+} concentration. The degree of Ca^{2+}-dependence approaches that observed in guinea-pig cerebral cortex but is much less than in rat cerebral cortex. Whether U373 MG cells will be of use as a model system for the apparent Ca^{2+}-entry component observed in guinea-pig or rat brain slices remains to be established.

Keywords: Histamine H_1-receptors; muscarinic M_3-receptors; calcium; inositol phosphates; U373 MG astrocytoma cells; HeLa cells; guinea-pig-brain; rat cerebral cortex

Introduction

There is now a body of evidence that histamine H_1-receptors in brain are associated with the 'arousal' response to histamine (Schwartz *et al.*, 1991), but the locus and cellular mechanisms involved remain uncertain. The primary cellular response to H_1-receptor activation appears to be G protein-mediated activation of phosphoinositidase C (PIC) (Hill, 1990) and in guinea-pig brain there is a good correlation between H_1-receptor density in different regions and histamine-stimulated inositol phosphate ([^{3}H]-IP) formation (Daum *et al.*, 1983). However, there are indications that there may be an additional pathway of phosphoinositide hydrolysis in brain. The most direct evidence is that in mouse and rat cerebral cortical slices, histamine-stimulated [^{3}H]-IP accumulation is almost linearly dependent on the Ca^{2+} content of the medium in the millimolar concentration range (Alexander *et al.*, 1990a), strongly suggesting the involvement of a Ca^{2+} entry step and Ca^{2+} activation of one or more PIC isoenzymes (Eberhard & Holz, 1988; Baird & Nahorski, 1990). Noradrenaline appears to be the only other monoamine to show this degree of Ca^{2+}-dependence of phosphoinositide breakdown in brain slices (Knepper & Rutledge, 1987; Alex-

[1] Author for correspondence.

ander *et al.*, 1990a) and in this case there is evidence for distinct α_1-adrenoceptor subtypes coupling with PIC and Ca^{2+} entry (Summers & McMartin, 1993), although the subtypes involved in [^{3}H]-IP formation in rat cerebral cortex remain uncertain (Michel *et al.*, 1990; Minneman & Atkinson, 1991). In contrast, carbachol-stimulated [^{3}H]-IP accumulation in mouse and rat cerebral cortex is essentially independent of extracellular Ca^{2+} above 0.3 mM (Alexander *et al.*, 1990a).

Histamine-activated Ca^{2+} channels or non-selective cation channels are well established in peripheral tissues such as intestinal smooth muscle cells (Komori *et al.*, 1992), endothelial cells (Yamamoto *et al.*, 1992) and adrenal medullary chromaffin cells (Goh & Kurosawa, 1991), and in the guinea-pig smooth muscle cells there is evidence that the non-selective cation channel is activated via a pertussis toxin-sensitive G protein (Komori *et al.*, 1992). However, there is no direct evidence for the presence of such channels in brain. A detailed investigation of the pathways of histamine-induced phosphoinositide metabolism in brain is hampered by the inherent complexity of brain slices and in particular by the presence of multiple cell types. There is thus a need for a simple model system. Ideally, two model systems are required: one which has only the direct H_1-receptor/G protein activation of PIC and a second with as large a contribution as possible from the presumed Ca^{2+} entry component. We have presented preliminary evidence that the human HeLa cell line may be a suitable model for the direct pathway (Arias-Montaño & Young, 1992), but finding a cell line of central origin as a model for the Ca^{2+}-dependent pathway has proved to be difficult. We describe here the characterization of histamine- and carbachol-induced inositol phosphate formation in human U373 MG astrocytoma cells and a comparison of the patterns of Ca^{2+}-dependence with those observed in HeLa cells and brain slices. To test for possible species differences in the latter we have compared the Ca^{2+}-dependence of histamine-induced [^{3}H]-IP_1 accumulation in slices from rat and guinea-pig cerebral cortex. In addition, since in rat cerebral cortex there is indirect evidence that H_1-receptors coupled to phosphoinositide hydrolysis are located, at least in part, on glial cells (Arbonés *et al.*, 1988), we have also made a comparison with guinea-pig cerebellum, where H_1-receptors are apparently predominantly neuronal (Palacios *et al.*, 1981).

Methods

Accumulation of [^{3}H]-inositol phosphates in U373 MG cells

U373 MG cells (National Culture Collection, Porton Down) were grown to near confluence in Dulbecco's modified Eagle medium (DMEM)/nutrient mixture F-12 (1:1 v/v; Gibco), containing 10% (v/v) bovine foetal calf serum and 2 mM glutamine (Gibco) and supplemented with penicillin (50 u ml^{-1}) and streptomycin (50 mg ml^{-1}) (Flow Laboratories), in flasks at 37°C in a CO_2-incubator (5% CO_2). The culture medium was removed and the cells washed in approximately 14 ml inositol-free DMEM before addition of inositol-free DMEM containing 10% dialysed calf serum, 10 μM *myo*-inositol and 2.5 μCi ml^{-1} [^{3}H]-inositol (0.16 μM). The cells were then incubated for 24 h. The [^{3}H]-inositol-labelled cells were washed once with approximately 15 ml phosphate buffered saline (PBS) (in mM: NaCl 137, KCl 2.7, Na_2HPO_4 8.1 and KH_2PO_4 1.5) containing 0.6 mM EDTA before dissociation with 10 ml trypsin/EDTA (500–750 BAEE units ml^{-1}/0.6 mM, Sigma). After centrifugation at 220 *g* for 5 min the cells were resuspended in Krebs-Henseleit medium (in mM: NaCl 116, KCl 4.7, $MgSO_4$ 1.2, KH_2PO_4 1.2, $NaHCO_3$ 25, $CaCl_2$ 2.5 and D-glucose 11). Cells (50 μl, approximately 8×10^5 cells) were added to 190 μl Krebs-Henseleit solution containing LiCl (final concentration 30 mM), gassed with O_2:CO_2 (95:5%), v/v, and incubated for 15 min at 37°C, before addition of 10 μl histamine or carbachol (final concentration 0.1–1000 μM). After each addition the tubes were gassed with O_2:CO_2 (95:5%, v/v) and the incubation continued at 37°C in a shaking water bath, usually for 30 min. Mepyramine or pirenzepine, where present, was added 15 min before the agonist. Incubations were terminated by addition of 250 μl of an ice-cold solution of 10% perchloric acid, containing 1 mM ethylenediaminetetraacetic acid (EDTA) and 1 mg ml^{-1} phytic acid, and allowed to stand on ice for 15 min. Inositol phosphates were extracted by the trioctylamine-freon method (Sharpes & McCarl, 1982; Downes *et al.*, 1986). Trioctylamine/1,1,2-trichlorotrifluoroethane (1:1, v/v) (0.4 ml) was added to the sample, the solution mixed thoroughly and then centrifuged at 950 *g* for 5 min to separate the phases. A sample (0.38 ml) of the upper phase was transferred to an insert vial, 4 ml 50 mM 2-amino-2-hydroxymethyl-propan-1,3-diol (Tris) buffer, pH 7.5, added and the mixture applied to an AG 1-X8 (formate form, 100–200 mesh; Biorad) anion-exchange column.

[^{3}H]-inositol and [^{3}H]-glycerophosphoinositol were eluted with 10 ml water and 10 ml 60 mM ammonium formate/5 mM sodium tetraborate, respectively, and [^{3}H]-inositol monophosphates ([^{3}H]-IP_1) then eluted with 10 ml 200 mM ammonium formate/100 mM formic acid. Higher phosphates were eluted by sequential addition of 10 ml 400 mM ammonium formate/100 mM formic acid (for [^{3}H]-inositol bisphosphates, [^{3}H]-IP_2) and 10 ml 800 mM ammonium formate/100 mM formic acid (for [^{3}H]-inositol trisphosphates, [^{3}H]-IP_3). This procedure does not separate individual mono-, bis-, and trisphosphate isomers. Thus the trisphosphate fraction will contain both 1,4,5- and 1,3,4-IP_3. Quicksafe A (10 ml, Zinnser) was added to each fraction and tritium determined by liquid scintillation counting. Within an experiment 3–4 replicate determinations were made of each incubation condition.

Accumulation of [^{3}H]-inositol phosphates in HeLa cells

HeLa cells (S3 clone) were grown to near confluence in DMEM (Gibco), containing 5% (v/v) bovine foetal calf serum and 5% (v/v) bovine neonate calf serum (Gibco) and supplemented with penicillin (50 u ml^{-1}) and streptomycin (50 mg ml^{-1}), in flasks at 37°C in a CO_2-incubator (5% CO_2). The culture medium was removed and the cells washed in approximately 14 ml inositol-free DMEM before addition of inositol-free DMEM containing 10% dialysed calf serum, 10 μM *myo*-inositol and 2.5 μCi ml^{-1} [^{3}H]-inositol (0.16 μM). Labelling of the cells, incubation with histamine and carbachol and extraction of [^{3}H]-inositol phosphates was carried out as described above. Antagonists were added 15 min before histamine or carbachol.

Accumulation of [^{3}H]-inositol phosphates in brain slices

Cross-chopped slices (350 × 350 μm, McIlwain tissue chopper) of guinea-pig (Dunkin-Hartley strain, males, 350–500 g; Tucks, Battlebridge, Essex) cerebellum and cerebral cortex and rat (Wistar strain, males, 200–350 g; Tucks, Battlebridge, Essex) cerebral cortex were washed three times and then incubated at 37°C for 60 min in Krebs-Henseleit medium with three further changes of medium. The medium was bubbled throughout with O_2/CO_2 (95:5, v/v). The slices were washed once more and then transferred to a flat-bottom vial (Hughes & Hughes, scintillation vial insert) and allowed to settle under gravity. Portions of the slices (30 μl) were added to 210 μl Krebs-Henseleit medium, containing 0.33 μM *myo*-[2-^{3}H]-inositol (1 μCi per incubation) and 10 mM LiCl, in insert vials. The mixture was incubated for 30 min in a shaking water bath before addition of 10 μl histamine or carbachol solution and further incubation for 60 min. Incubations were terminated and [^{3}H]-inositol phosphates determined as described under U373 MG cells above.

Ca^{2+}-dependence of [^{3}H]-inositol phosphate accumulation

In experiments on the Ca^{2+}-dependence of histamine- or carbachol-induced [^{3}H]-inositol phosphate accumulation, brain slices were preincubated in normal Krebs-Henseleit and then labelled with [^{3}H]-inositol and exposed to agonist in medium containing the concentration of Ca^{2+} under test. U373 MG and HeLa cells were labelled with [^{3}H]-inositol and dissociated following the standard protocol (see above). The dissociated cells were washed twice in Krebs-Henseleit solution from which Ca^{2+} had been omitted and then equilibrated for 15 min in Krebs-Henseleit solution containing the Ca^{2+} concentration under test. Further incubation with or without 1 mM histamine or 1 mM carbachol was for 30 min. For '0 Ca^{2+}', Ca^{2+} was omitted from the medium.

Measurement of [^{3}H]-mepyramine binding to U373 MG cell membranes

U373 MG cells were lysed in 50 mM Na-K phosphate buffer (37.8 mM Na_2HPO_4, 12.2 mM KH_2PO_4), pH 7.5, and centrifuged at *circa* 15,000 *g* for 10 min. The pellet was resuspended in buffer and recentrifuged at *circa* 15,000 *g* for 10 min. The final pellet was resuspended in buffer and stored at − 20°C. When required, pellets were thawed and homogenized in a teflon-glass homogenizer with a motor-driven pestle (300 r.p.m., 10 up and down strokes) and resuspended in buffer. Protein was measured essentially as described by Lowry *et al.* (1951).

Incubations in 50 mM Na-K phosphate buffer, pH 7.5, contained [^{3}H]-mepyramine (0.3–20 nM) and U373 MG cell membrane homogenate (0.19–0.23 mg protein) in a final volume of 1.0 ml (3–4 replicates at each concentration). A parallel set of incubations contained in addition 1 μM temelastine to define non-H_1-receptor binding. Incubation was for 60 min at 30°C and was terminated by filtration through Whatman GF/B glass fibre paper, pre-soaked in 0.3% (w/v) polyethylenimine for 3–5 h, using a Brandel (Gaithersburg, Md, U.S.A.) cell harvester. The filters were washed with ice-cold buffer and then transferred to scintillation insert vials and 4.0 ml Emulsifier-Safe scintillator (Packard) added. The vials were allowed to stand at room temperature for at least 2 h before counting.

Analysis of data

Concentration-response data for agonist-induced [^{3}H]-IP_1 accumulation (after subtraction of basal accumulation) were fitted to a Hill equation (logistic equation) using the Harwell Library non-linear regression programme VB01A. The actual equation fitted was:

$$[^3H]\text{-}IP_1 \text{ accumulated} = Resp_{max}.C^n/(C^n + EC_{50}^n)$$

where C is the agonist concentration, EC_{50} is the concentration giving the half-maximal response, n is the Hill coefficient and $Resp_{max}$ is the maximum response. Each point was weighted according to the reciprocal of the variance associated with it. Curves of the temelastine-sensitive binding of [^{3}H]-mepyramine *versus* the concentration of [^{3}H]-mepyramine were analysed similarly to obtain best-fit values of the Hill coefficient. Since the Hill coefficient was not significantly different from unity in any of the three experiments, the data were fitted to a hyperbola (n = 1 in the equation above) to obtain the EC_{50} (= K_d) and B_{max}.

Statistical comparison of parameters characterizing two concentration-response curves was made by fitting the curves simultaneously (using the NAG library routine E04FDF) and assessing the increase in the residual sum of squares when

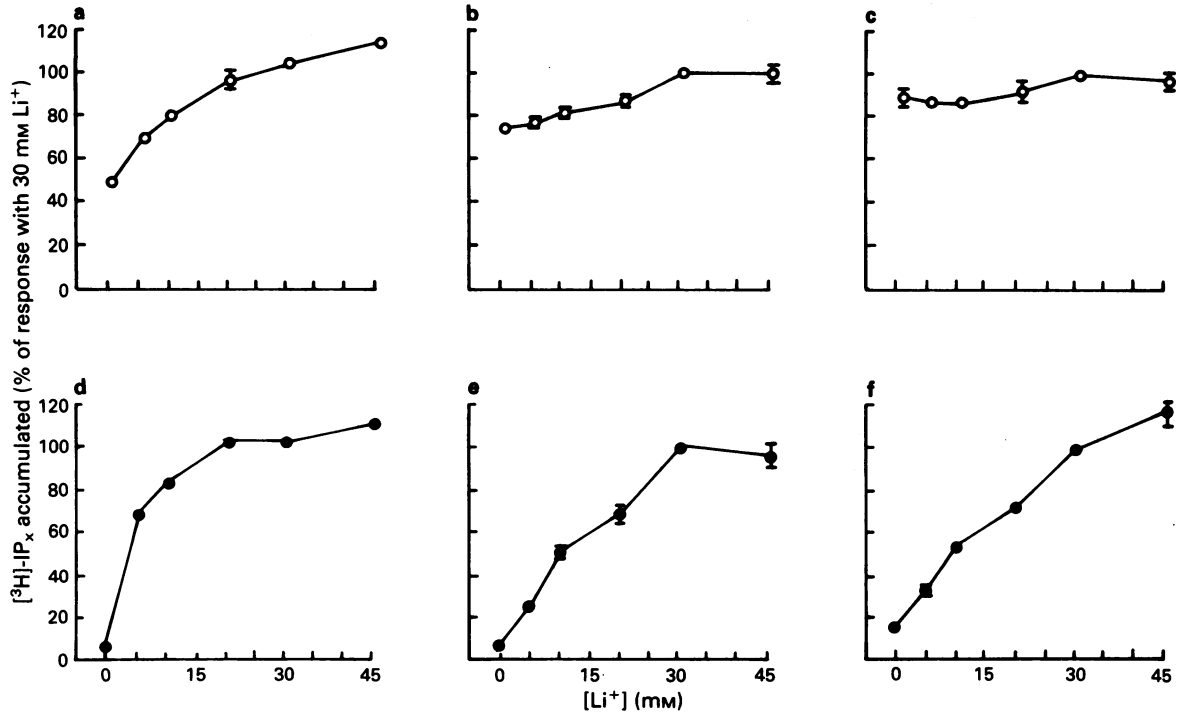

Figure 1 Sensitivity of basal and histamine-induced [^{3}H]-IP_1, [^{3}H]-IP_2 and [^{3}H]-IP_3 accumulation to Li^+. U373 MG cells were incubated with the test concentration of Li^+ for 15 min before incubation for 30 min in the presence or absence (basal) of 1 nM histamine. Values are the weighted means ± s.e.mean from three experiments. To allow for variation in the absolute magnitude of the response between experiments, accumulations in the presence of 30 mM Li^+ were set at 100%. Where no error bars are shown the error was within the size of the symbol. Mean basal accumulations (○) in the presence of 30 mM Li^+ were: [^{3}H]-IP_1 (a) 1,305 ± 16 d.p.m., [^{3}H]-IP_2 (b) 880 ± 9 d.p.m., and [^{3}H]-IP_3 (c) 320 ± 13 d.p.m. Corresponding accumulations induced by 1 mM histamine (basal accumulation subtracted) (●) were: [^{3}H]-IP_1 (d) 18,642 ± 131 d.p.m., [^{3}H]-IP_2 (e) 3,353 ± 89 d.p.m., and [^{3}H]-IP_3 (f) 938 ± 20 d.p.m.

parameters were constrained to be the same for both curves, by calculating the *F*-statistic (Rodbard, 1974):

$$F = \{(SS_2 - SS_1)/(df_2 - df_1)\}/(SS_1/df_1)$$

where SS_2 is the sum of squares when a parameter is shared (df_2 degrees of freedom) and SS_1 the sum of squares when all parameters are allowed to float freely for each curve (df_1 degrees of freedom).

The dissociation constants for mepyramine and pirenzepine in U373 MG cells were determined from shifts of the concentration-response curve for histamine- or carbachol-induced [^{3}H]-IP$_1$ accumulation using the relationship: log (concentration-ratio − 1) = log([A]) − log(K_d), where the concentration-ratio is the ratio of the EC_{50} values in the presence and absence of antagonist, [A] is the concentration of the antagonist and K_d its dissociation constant. Unbiased estimates of the concentration-ratio were obtained from best-fit EC_{50} values by fitting simultaneously (using the E04FDF routine as above) curves in the presence and absence of a single concentration of mepyramine or pirenzepine, measured in the same experiment, with the Hill slope and the maximum response constrained to be the same for both curves. This obviates difficulties with shifted curves where the maximum response is poorly defined. Where individual curves could be fitted satisfactorily without constraints, constraining Hill coefficients and maximum responses did not significantly worsen the fit.

Multiple comparisons of values at different times or under different incubation conditions within a single experiment were made using the Student-Newman-Keuls multiple range test.

Drugs

Myo-[2-^{3}H]-inositol, 20–24 Ci mmol^{-1}, was obtained from New England Nuclear and [*pyridinyl*-5-^{3}H]-mepyramine, 21 Ci mmol^{-1}, from Amersham International. Adenosine, carbachol (carbamylcholine chloride), histamine dihydrochloride, mepyramine maleate, N-methylatropine bromide, phytic acid, pirenzepine hydrochloride, prazosin hydrochloride and ω-conotoxin GVIA were purchased from Sigma; 1,1,2-trichlorotrifluoroethane (freon) and tri-n-octylamine from Aldrich. Temelastine was kindly provided by Smith, Kline & French Research Ltd and nimodipine by Dr K. Byron, University of Cambridge.

Results

Lithium-sensitivity of histamine-induced [^{3}H]-IP$_x$ accumulation in U373 MG cells

Basal accumulation of [^{3}H]-IP$_1$ in U373 MG cells, measured 45 min after addition of Li^+, increased as the concentration of Li^+ present was increased from 0 to 45 mM (Figure 1a). The accumulations of [^{3}H]-IP$_2$ and [^{3}H]-IP$_3$ were much less affected (Figure 1b,c). However, accumulations of all three fractions induced by incubation with 1 mM histamine for 30 min were much more sensitive to Li^+ than the corresponding basal accumulations. Histamine-induced accumulation of [^{3}H]-IP$_1$ appeared to reach a plateau level at approximately 20 mM Li^+ (Figure 1d), whereas the accumulation of [^{3}H]-IP$_3$ increased throughout the range 0 to 45 mM Li^+ (Figure 1f) and that of [^{3}H]-IP$_2$ only appeared to have reached a maximum level at 45 mM Li^+ (Figure 1e). Since [^{3}H]-IP$_1$ is present in the greatest amounts (see below), all subsequent incubations were carried out with 30 mM Li^+ present.

Characterization of histamine-induced [^{3}H]-IP$_x$ accumulation in U373 MG cells

In the presence of 1 mM histamine and 30 mM Li^+ the accumulation of [^{3}H]-IP$_1$ increased with time over the period studied (Figure 2a), whereas the accumulations of [^{3}H]-IP$_2$ and [^{3}H]-IP$_3$ initially increased rapidly, but had reached a maximum by 10 and 5 min, respectively (Figure 2b and 2c). Basal levels of [^{3}H]-IP$_1$, but not [^{3}H]-IP$_2$ and [^{3}H]-IP$_3$, increased slightly, but significantly, over the 60 min. In all subsequent experiments the period of incubation with histamine was 30 min. Under these conditions [^{3}H]-IP$_1$ accounts for 84 ± 1% of total [^{3}H]-IP$_1$ + [^{3}H]-IP$_2$ + [^{3}H]-IP$_3$ (nine determinations). The mean accumulation of [^{3}H]-IP$_1$ in the presence of 1 mM histamine was 11 (± 1) fold of basal accumulation ($n = 31$). There was no indication of any change in the extent of the response to histamine with passage number (up to 40). The EC_{50} for histamine-induced accumulation was 5.4 ± 0.5 μM (best-fit value to the combined data from 15 determinations; best-fit value of the Hill coefficient 0.89 ± 0.06).

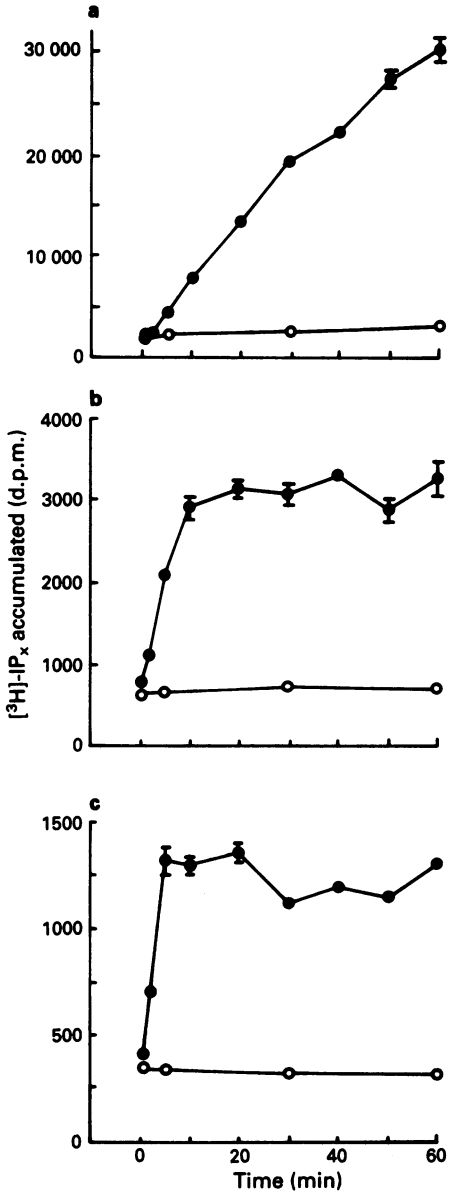

Figure 2 Time course of [^{3}H]-IP$_x$ accumulation in the presence and absence of 1 mM histamine. Incubation with 1 mM histamine was for 30 min. Values are the means ± s.e.mean from triplicate determinations from a single experiment. Where no error bars are shown the error was within the size of the symbol. The whole experiment was repeated three times with similar results. (a) [^{3}H]-IP$_1$, (b) [^{3}H]-IP$_2$, (c) [^{3}H]-IP$_3$. (○) No addition (basal); (●) + 1 mM histamine.

Concentration-response curves for histamine-induced [^{3}H]-IP_1 accumulation were displaced to the right in a parallel fashion by increasing concentrations of mepyramine (Figure 3a). A Schild plot of the data from 11 experiments with 10–100 nM mepyramine was linear with a slope of 0.99 ± 0.08 (Figure 3b). Log K_d derived from this plot was 8.46 ± 0.03 (K_d 3.5 ± 0.3 nM, approximate s.e.mean).

[^{3}H]-mepyramine binding to U373 MG cell membranes

The binding of [^{3}H]-mepyramine insensitive to inhibition by 1 μM temelastine (non-H_1-receptor binding) increased linearly with the concentration of [^{3}H]-mepyramine between 0.4 and 20 nM. The non-specific binding accounted for 30–45% of the total binding at 2 nM and 70–77% of the total binding at 20 nM [^{3}H]-mepyramine (three experiments). The Hill coefficients of the curves of the temelastine-sensitive binding of [^{3}H]-mepyramine did not differ significantly from unity. The maximum H_1-receptor binding was 78 ± 12, 122 ± 5 and 59 ± 4 pmol g^{-1} protein in the three experiments, with corresponding EC_{50} (K_d) values of 2.1 ± 0.5, 4.3 ± 0.5 and 1.0 ± 0.2 nM, respectively (mean 2.5 ± 1.0 nM). The error on the mean K_d is appreciable, but the value is in reasonable accord with the value of 3.5 ± 0.3 nM obtained from inhibition of histamine-induced [^{3}H]-IP_1 accumulation.

Characteristics of carbachol-induced [^{3}H]-IP_x accumulation in U373 MG cells

Carbachol also stimulated [^{3}H]-IP_1 accumulation in U373 MG cells, with a time-course similar to that observed for histamine, although the extent of the accumulation was less, 2.8 (± 0.1) fold of basal in the presence of 1 mM carbachol (n = 17). [^{3}H]-IP_1 was again much the major labelled product under these conditions (88 ± 1% of total [^{3}H]-IP_1 + [^{3}H]-IP_2 + [^{3}H]-IP_3, seven determinations).

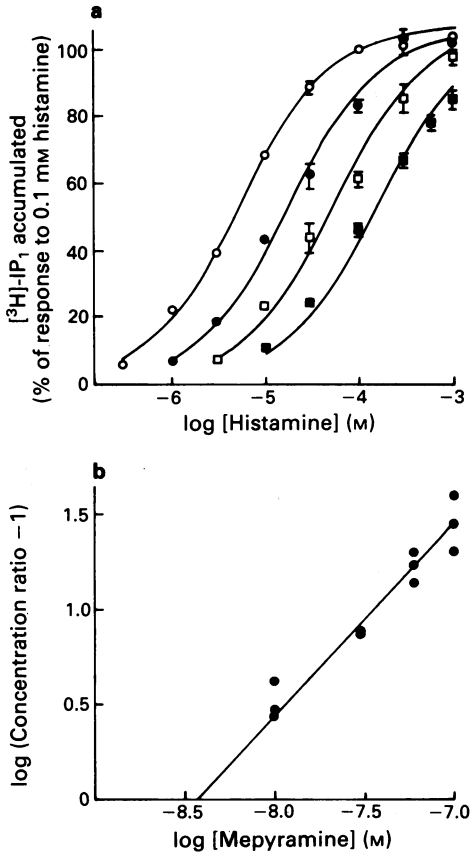

Figure 3 Inhibition of histamine-induced [^{3}H]-IP_1 accumulation by mepyramine. (a) Values are the weighted means ± s.e.mean from the combined data from 11 curves for histamine, two curves with 3 nM mepyramine and three curves with 10 and 100 nM mepyramine. To allow for variations in the absolute magnitude of the accumulation of [^{3}H]-IP_1 between experiments, the data have been normalised by setting the response in the presence of 100 μM histamine to 100%. Where no error bars are shown the error was within the size of the symbol. The lines drawn are the best-fit curves with maximum values and Hill coefficients constrained to a common value (see Methods). (○) Histamine alone; (●) + 10 nM mepyramine; (□) + 30 nM mepyramine; (■) + 100 nM mepyramine. (b) Schild plot of the data for mepyramine. Each point is an unbiased estimate of the concentration-ratio obtained from the ratio of the EC_{50} values obtained by fitting simultaneously concentration-response curves for histamine and histamine + 10, 30, 60 or 100 nM mepyramine measured in the same experiment, with the Hill coefficient and the maximum response constrained to be the same for both curves (see Methods). For clarity the error bars (estimated error) have been omitted. The line drawn was calculated by linear regression analysis. Best-fit values: slope 0.99 ± 0.08, intercept (log affinity constant) 8.46 ± 0.03.

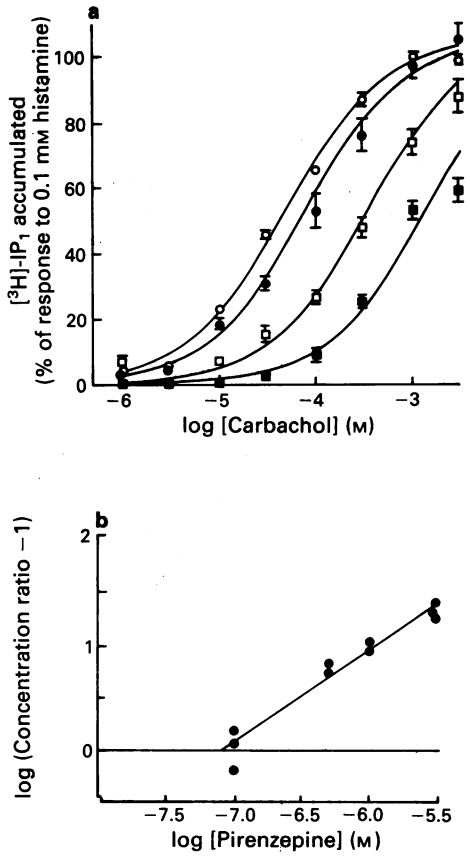

Figure 4 Inhibition of carbachol-induced [^{3}H]-IP_1 accumulation by pirenzepine. (a) Values are the weighted means ± s.e.mean from the combined data from 10 curves for carbachol, three curves with 100 nM and 3 μM pirenzepine and two curves with 1 μM pirenzepine. To allow for variations in the absolute magnitude of the accumulation of [^{3}H]-IP_1 between experiments, the data have been normalised by setting the response in the presence of 1 mM carbachol to 100%. Where no error bars are shown the error was within the size of the symbol. The lines drawn are the best-fit curves with maximum values and Hill coefficients constrained to a common value (see Methods). (○) Carbachol alone; (●) + 100 nM pirenzepine; (□) + 1 μM pirenzepine; (■) + 3 μM pirenzepine. (b) Schild plot of the data for pirenzepine. Each point is an unbiased estimate of the concentration-ratio obtained from the ratio of the EC_{50} values obtained by fitting simultaneously concentration-response curves for carbachol and carbachol + 100 nM, 500 nM, 1 μM and 3 μM pirenzepine measured in the same experiment, with the Hill coefficient and the maximum response constrained to be the same for both curves (see Methods). The error bars have been omitted for clarity. The line drawn was calculated by linear regression analysis. Best-fit value of the slope 0.89 ± 0.07.

Concentration-response curves for carbachol-induced [^{3}H]-IP_1 accumulation, EC_{50} 48 ± 8 μM and Hill coefficient of 0.85 ± 0.07 (best-fit values ± approximate s.e. to the combined data from 12 determinations), were displaced to the right by pirenzepine (Figure 4a). A Schild plot of the data (Figure 4b) had a slope, 0.89 ± 0.07, not significantly different from unity. Constraining the slope to be unity yielded a log K_d of 7.0 ± 0.01 (K_d 1.01 ± 0.04 × 10^{-7} M, approximate s.e.), a value in the range expected for binding to the M_3-muscarinic receptor subtype (Hulme *et al.*, 1990).

Ca^{2+}-dependence of histamine- and carbachol-induced [^{3}H]-IP_x accumulation in U373 MG cells

[^{3}H]-IP_1, [^{3}H]-IP_2 and [^{3}H]-IP_3 accumulations in the presence of 1 mM histamine increased markedly as the Ca^{2+} concentration in the medium was increased from nominally zero (no added Ca^{2+}) to 0.3 mM, followed by less pronounced, but statistically significant ($P<0.05$, Student-Newman-Keuls multiple range test), increases as extracellular Ca^{2+} was increased to 1.3 mM and from 1.3 to 4.0 mM (Figure 5). The pattern of the Ca^{2+}-dependence was similar for all three fractions. There was a small, statistically significant, increase in basal [^{3}H]-IP_1 and [^{3}H]-IP_2 accumulation between no added Ca^{2+} and 0.3 mM Ca^{2+}, but a further increase in the concentration of Ca^{2+} in the medium had no added effect (Figure 5). The relative amount of [^{3}H]-IP_1 induced by 1 mM histamine, expressed as a percentage of [^{3}H]-IP_1 + [^{3}H]-IP_2 + [^{3}H]-IP_3 accumulated, did not differ significantly at 2.5 mM Ca^{2+}, 84 ± 1% (9), and 4.0 mM Ca^{2+}, 85 ± 1% (4).

Carbachol-induced accumulation of [^{3}H]-IP_1, [^{3}H]-IP_2 and [^{3}H]-IP_3 also increased between 'zero' and 0.3 mM Ca^{2+} (Figure 6). There was an additional increase in [^{3}H]-IP_1 and [^{3}H]-IP_2 accumulation as the Ca^{2+} was increased to 1.3 mM, but further increase to 4 mM had no significant effect on the amount of [^{3}H]-IP_1 and caused a decrease in [^{3}H]-IP_2. Amounts of [^{3}H]-IP_3 accumulated were very small (Figure 6c), but there was no indication of the stimulatory effect of increasing the extracellular Ca^{2+} from 0.3 to 4 mM seen with the response to histamine (Figure 5).

Ca^{2+}-dependence of histamine- and carbachol-induced [^{3}H]-IP_x accumulation in HeLa cells

Histamine (1 mM) induced an accumulation of [^{3}H]-IP_1 8.03 (± 0.08) fold (17) of basal level in the HeLa S3 clone. This is approximately 4 fold greater than the magnitude of the response to histamine in the unspecified clone used in our earlier study with HeLa cells (Bristow *et al.*, 1991). In

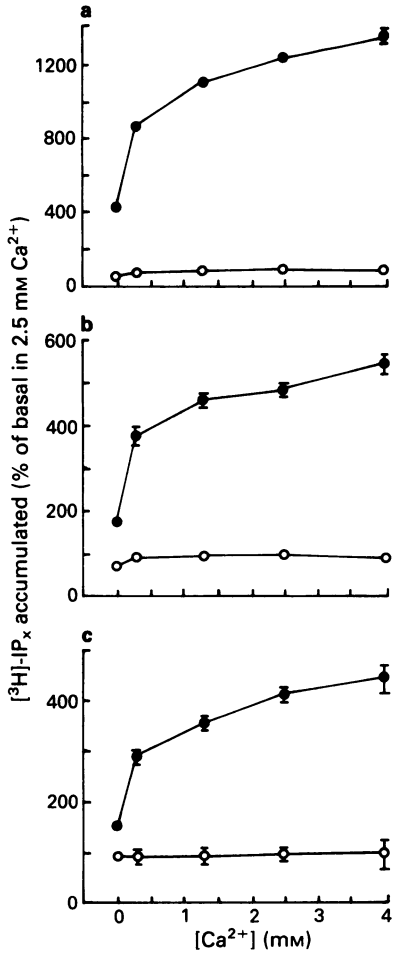

Figure 5 Ca^{2+}-dependence of histamine-induced [^{3}H]-IP_x accumulation. Values are the weighted means ± s.e.mean from 3 experiments. To allow for differences in the absolute magnitude of the accumulation between experiments, values have been expressed as a percentage of basal acccumulation of each isomer in the presence of 2.5 mM Ca^{2+}. (a) [^{3}H]-IP_1; (b) [^{3}H]-IP_2; (c) [^{3}H]-IP_3 (mean basal accumulations at 2.5 mM Ca^{2+} 1187 ± 11, 465 ± 9 and 260 ± 9 d.p.m., respectively). Where no error bar is shown the error was within the size of the symbol. (○) No addition (basal); (●) + 1 mM histamine.

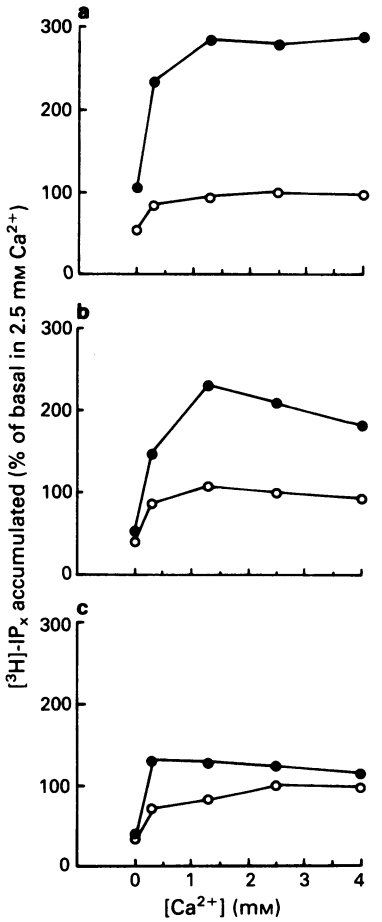

Figure 6 Ca^{2+}-dependence of carbachol-induced [^{3}H]-IP_x accumulation. Values are the weighted means ± s.e.mean from 4 experiments. To allow for differences in the absolute magnitude of the accumulation between experiments, values have been expressed as a percentage of basal acccumulation of each isomer in the presence of 2.5 mM Ca^{2+}. (a) [^{3}H]-IP_1; (b) [^{3}H]-IP_2; (c) [^{3}H]-IP_3 (mean basal accumulations at 2.5 mM Ca^{2+} 808 ± 7, 357 ± 5 and 264 ± 5 d.p.m., respectively). Where no error bar is shown the error was within the size of the symbol. (○) No addition (basal); (●) + 1 mM carbachol.

occasional experiments the response to 1 mM histamine was as much as 14–20 fold of basal, without there being any appreciable change in the basal accumulation. In one experiment in which the response to 1 mM histamine was 19 fold of basal, the concentration-response curve to histamine (EC_{50} 11.3 ± 1.1 μM, Hill coefficient 0.93 ± 0.04) appeared to be shifted somewhat to higher concentrations compared with curves in cells showing the normal, approximately 8 fold, stimulation (EC_{50} 3.9 ± 0.7 μM, Hill coefficient 0.68 ± 0.08; best-fit values to the combined data from a total of 18 experiments). The properties of the histamine response in the S3 clone, where tested, appeared to be the same as in the unspecified clone used earlier and in particular showed the same lower sensitivity of [^{3}H]-IP_1 accumulation to Li^+ (Bristow *et al.*, 1991) than in brain slices or U373 MG cells. The proportion of [^{3}H]-IP_1 as a percentage of [^{3}H]-IP_1 + [^{3}H]-IP_2 + [^{3}H]-IP_3 after a 30 min incubation with 1 mM histamine in the presence of 30 mM Li^+ was 92 ± 1% (16).

Carbachol also stimulated [^{3}H]-IP_1 accumulation in the S3 clone and the extent of the stimulation, 3.9 (± 0.1) fold of basal (6), was again greater than in the unspecified clone used earlier, 1.8 (± 0.1) fold of basal (10). The concentration-response curve for carbachol-induced [^{3}H]-IP_1 formation (EC_{50} 21 ± 4 μM, Hill coefficient 1.22 ± 0.31; best-fit values to the combined data from a total of 11 experiments) was shifted to the right by 100 nM and 1 μM pirenzepine, but in this series of experiments the fit to the combined data was significantly worsened when the Hill coefficient and the maximum attainable response were constrained to be the same in the presence and absence of pirenzepine (see Analysis of data under Methods). However, the apparent K_d values derived for pirenzepine, 1.0×10^{-7} M and 0.84 ± 10^{-7} M, indicate the probable presence of the M_3-muscarinic receptor subtype (Hulme *et al.*, 1990).

The pattern of Ca^{2+}-dependence of [^{3}H]-IP_1 accumulation induced by 1 mM histamine in HeLa cells was closely similar to that for the response to 1 mM carbachol (Figure 7). After the initial increase between 'zero' and 0.3 mM Ca^{2+} the response to histamine was not significantly altered as the Ca^{2+} in the medium was increased to 4.0 mM. The response to carbachol did increase significantly between 0.3 and 1.3 mM Ca^{2+}, but there was no further increase at higher Ca^{2+} concentrations. Basal [^{3}H]-IP_1 accumulation also increased between 0 (nominal) and 0.3 mM Ca^{2+}, but remained unchanged thereafter (Figure 7). The same pattern of Ca^{2+}-dependence of basal and histamine-stimulated [^{3}H]-IP_1 accumulation as in the S3 clone was observed in 4 experiments with the clone of HeLa cells showing the lower stimulation with histamine (data not shown).

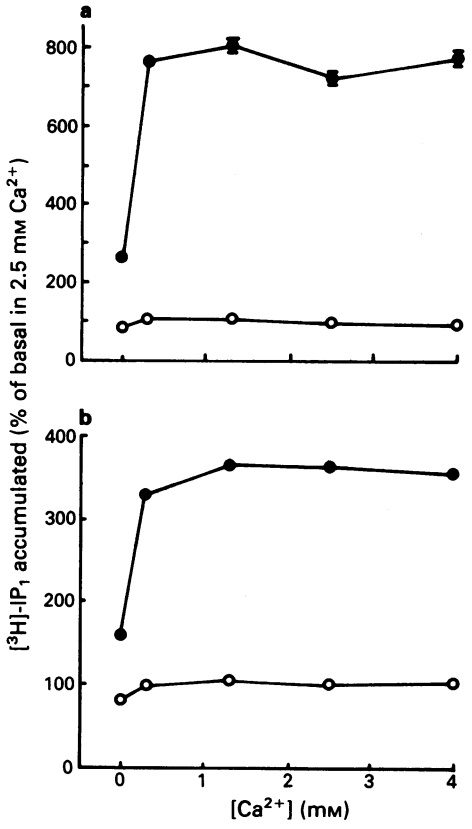

Figure 7 Ca^{2+}-dependence of histamine- and carbachol-induced [^{3}H]-IP_1 accumulation in HeLa cells (S3 clone). Cells were labelled with [^{3}H]-inositol and dissociated following the standard protocol (see Methods). The dissociated cells were equilibrated for 15 min and incubated with or without 1 mM histamine (a) or 1 mM carbachol (b) for 30 min in Krebs-Henseleit solution containing the Ca^{2+} concentration under test. For '0 Ca^{2+}', Ca^{2+} was omitted from the medium. Points are the combined values from 4 experiments with histamine and three experiments with carbachol and are expressed as a percentage of the 30 min basal value in 2.5 mM Ca^{2+} (3276 ± 49 and 2339 ± 75 d.p.m. in the two sets of experiments, respectively) to allow for differences in the absolute magnitude of the response between experiments. (○) Basal; (●) 1 mM histamine (a) or 1 mM carbachol (b).

Ca^{2+}-dependence of [^{3}H]-IP_1 accumulation in rat and guinea-pig brain slices

Basal accumulation of [^{3}H]-IP_1 in rat and guinea-pig cerebral cortical slices and in guinea-pig cerebellar slices was not significantly altered, except at 4.0 mM Ca^{2+} in rat cerebral cortex, when slices were labelled with [^{3}H]-inositol and incubated in Krebs-Henseleit solutions with no added Ca^{2+} or with Ca^{2+} concentrations from 0.3 to 4.0 mM (Figure 8a). In contrast, [^{3}H]-IP_1 accumulation induced by 1 mM histamine in rat cerebral cortical slices increased markedly with the Ca^{2+} concentration, in agreement with the previously reported Ca^{2+}-dependence of histamine-induced [^{3}H]-IP accumulation in mouse cerebral cortex (Alexander *et al.*, 1990a,b). Amounts of [^{3}H]-IP_2 and [^{3}H]-IP_3 were much less than those of [^{3}H]-IP_1, but the pattern of Ca^{2+}-dependence was essentially the same as that for [^{3}H]-IP_1 (data not shown).

Histamine-induced [^{3}H]-IP_1 accumulation in guinea-pig cerebellar slices, a tissue relatively rich in H_1-receptors (Hill *et al.*, 1978), was also Ca^{2+}-dependent, but the pattern of the Ca^{2+}-dependence differed from that in rat cerebral cortex, in that there was a marked increase in the response between no added Ca^{2+} and 0.3 mM Ca^{2+}, followed by a less steep increase to 2.5 mM Ca^{2+} (Figure 8c). There was no further increase between 2.5 and 4.0 mM. The pattern of histamine-induced [^{3}H]-IP_2 accumulation was similar, whereas amounts of [^{3}H]-IP_3 appeared to decrease between 2.5 and 4.0 mM (data not shown). The Ca^{2+}-dependence of the histamine response in guinea-pig cerebral cortical slices was intermediate between that of rat cerebral cortex and that of guinea-pig cerebellum (Figure 8b).

The Ca^{2+}-dependence of carbachol-induced [^{3}H]-IP_1 accumulation was similar in rat cerebral cortex and in guinea-pig cerebral cortex and in both tissues differed from that for histamine (Figure 8d,e). The pattern observed, an initial increase between 0 (nominal) and 0.3 mM Ca^{2+} but no further increase (up to 4.0 mM Ca^{2+}), is similar to that reported for carbachol-induced [^{3}H]-IP accumulation in mouse cerebral cortex (Alexander *et al.*, 1990a). The Ca^{2+}-dependence of carbachol-induced [^{3}H]-IP_2 and [^{3}H]-IP_3 accumulation in rat cerebral cortex was similar to that for [^{3}H]-IP_1, except that 1.3 mM Ca^{2+} was required to obtain the maximum amount of [^{3}H]-IP_3.

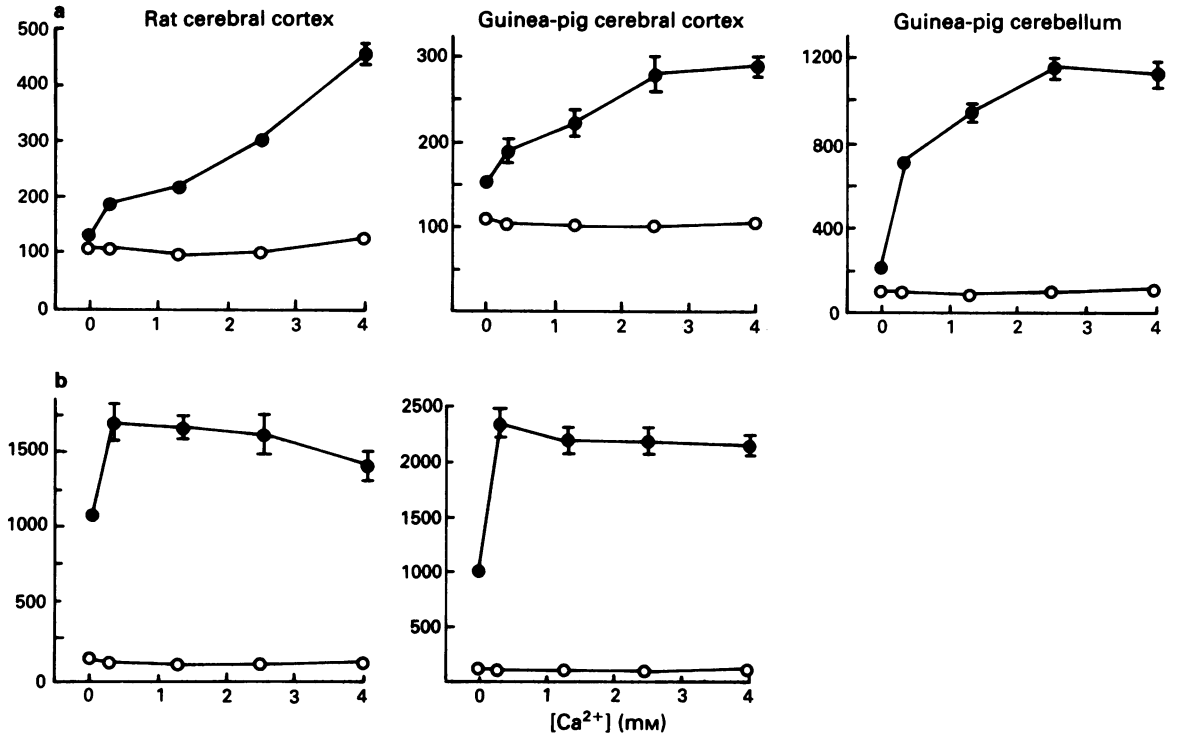

Figure 8 Ca^{2+}-dependence of histamine- and carbachol-induced [^{3}H]-IP_1 accumulation in rat and guinea-pig brain slices; (a) histamine, (b) carbachol. Slices were preincubated in normal Krebs-Henseleit and then labelled with [^{3}H]-inositol and incubated with or without (basal) agonist in Krebs-Henseleit solution containing the Ca^{2+} concentration indicated. Incubations with 1 mM histamine or 1 mM carbachol were for 60 min. Points are weighted means ± approximate s.e.mean from 3 or 4 independent determinations and are expressed as a percentage of the 30 min basal value with 2.5 mM Ca^{2+} to allow for differences in the absolute magnitude of the responses between experiments. Mean basal accumulation in 2.5 mM Ca^{2+} were 1583 ± 12 (37) in rat cerebral cortex, 926 ± 7 (11) in guinea-pig cerebral cortex and 3479 ± 71 (8) in guinea-pig cerebellum. (○) Basal; (●) 1 mM histamine (a) or 1 mM carbachol (b).

Effect of nimodipine and ω-conotoxin on histamine-induced [^{3}H]-IP_1 accumulation

Blockade of L-type Ca^{2+} channels with 100 nM nimodipine did not inhibit [^{3}H]-IP_1 accumulation induced by 1 mM histamine in the presence of 2.5 mM Ca^{2+} in rat cerebral cortical slices (104 ± 9% of the response in the absence of antagonist, $n = 3$) or in U373 MG cells (102 ± 2%, $n = 4$), the two preparations showing a calcium-dependence of the histamine response. Nimodipine was similarly ineffective against histamine in slices of guinea-pig cerebral cortex and cerebellum (94 ± 4% and 98 ± 6% of control, respectively; $n = 3$). Blockade of N-type Ca^{2+} channels by ω-conotoxin (0.1–3 μM) also failed to have any significant effect on [^{3}H]-IP_1 accumulation induced by 1 mM histamine in rat cerebral cortical slices (103 ± 8% of control with 3 μM ω-conotoxin, $n = 3$) or in U373 MG cells (104 ± 2%, $n = 4$).

The lack of effect of blockade of N-type Ca^{2+} channels suggests that the Ca^{2+}-dependence of the response to histamine in rat cerebral cortical slices is not likely to be due to H_1-receptor-mediated release of a secondary stimulator of phosphoinositidase C. Acetylcholine and noradrenaline are apparently not involved, since N-methylatropine (1 μM) and prazosin (1 μM) had no significant effect on [^{3}H]-IP_1 accumulation induced by 1 mM histamine in the slices (105 ± 7% and 96 ± 5%, respectively, of the response to histamine alone, $n = 3$).

Discussion

The relatively large magnitude of histamine H_1-receptor-induced phosphoinositide hydrolysis in U373 MG human astrocytoma cells, 11 fold of basal levels, compared with the response to histamine in most other cell types makes them attractive as a model system on which to study H_1-receptor function. However, how good a model the U373 MG cells are of the apparent Ca^{2+}-dependent component of the response to histamine apparent in slices of mouse and rat cerebral cortex (Alexander *et al.*, 1990a) is less clear. One particular problem in making a judgement is that in most brain regions there is little indication which cell type or types are responding to histamine. In the molecular layer of guinea-pig cerebellum autoradiographic studies of the effect of kainic acid lesions on the binding of [^{3}H]-mepyramine suggest that H_1-receptors have a neuronal location, presumably on the dendrites of Purkinje cells (Palacios *et al.*, 1981). A neuronal location of some H_1-receptors is also indicated by the observation of histamine-induced [^{3}H]-IP accumulation in primary cultures of striatal neurones, although the magnitude of the response was modest (Weiss *et al.*, 1988). However, neither kainic acid nor lesioning of the medial forebrain bundle in rats caused any persistent decrease in the binding of [^{3}H]-mepyramine to hippocampal membranes and the conclusion was drawn that the majority of hippocampal H_1-receptors were on glial cells (Chang *et al.*, 1980). Cerebral microvessels also possess histamine H_1-receptors (Peroutka *et al.*, 1980), but it has been estimated that they account for less than 1% of total cerebral H_1-receptors (Culvenor & Jarrott, 1981).

More direct evidence for a glial cell location is provided by the presence of histamine H_1-receptors on primary cultures of astrocytes from neonate rat brain, as evidenced both by [^{3}H]-mepyramine binding (Inagaki *et al.*, 1989) and by histamine-stimulated [^{3}H]-IP accumulation (Arbonés *et al.*, 1988). More specifically, Wada and his collaborators have

demonstrated that phosphoinositide hydrolysis in response to histamine is localized to type-2 astrocytes (Kondou *et al.*, 1991) and that Ca^{2+} signals induced by H_1-receptor activation can first be detected on the process of these cells (Inagaki *et al.*, 1991). Functionally, astrocytes are a major site of glycogen storage in the CNS (Murphy & Pearce, 1987) and H_1-receptor-mediated stimulation of glycogenolysis has been demonstrated in primary cultures of astrocytes (Arbonés *et al.*, 1990). It therefore seems probable that the glycogen breakdown induced by H_1-receptor activation in slices of mouse cerebral cortex (Quach *et al.*, 1980) reflects the presence of functional H_1-receptors on astrocytes in cerebral cortex *in vivo*. A strong argument can thus be made for astrocyte-derived cell lines as model systems for the study of H_1-receptor mechanisms in mammalian CNS.

Functional responses to H_1-receptor activation have been reported in the 1321N1 and UC11 MG human astrocytoma cell lines (Nakahata *et al.*, 1986; Medrano *et al.*, 1992; Lucherini & Gruenstein, 1992) and Johnson & Johnson (1992) noted, without presenting any experimental detail, that histamine-induced formation of [^{3}H]-IP_1 could be detected in UC11 MG cells, but that it was less than that in U373 MG cells. The data presented in the present study provide evidence that histamine does induce a large accumulation of [^{3}H]-IP_1 in U373 MG cells and that the effect is mediated by an H_1-receptor. Moreover, there is a clear dependence of the magnitude of the response to histamine on the extracellular Ca^{2+} concentration, even after the initial step to 0.3 mM Ca^{2+} (Figure 5). The marked inhibition of histamine-induced [^{3}H]-IP formation if Ca^{2+} is omitted from the medium is well established, both in brain slices (Kendall & Nahorski, 1984) and in primary cultures of astrocytes (Arbonés *et al.*, 1988) and is not confined to the H_1-receptor, as is evident with the response to carbachol in brain slices (Alexander *et al.*, 1990a; Figure 8d), HeLa cells (Figure 7) and U373 MG cells (Figure 6). However, it is the marked effect of increasing the Ca^{2+} concentration in the millimolar range which is the striking feature of the response to histamine in rat cerebral cortex (Figure 8d) and the same characteristic is shown, although to a lesser degree, by the U373 MG cells (Figure 5). The possibility that the effect of Ca^{2+} reflects an action on histamine binding to the H_1-receptor, rather than some aspect of the mechanism of phosphoinositide hydrolysis, is made unlikely by comparison with the Ca^{2+}-dependence of [^{3}H]-IP_1 formation induced by histamine in HeLa cells (Figure 7).

Histamine-stimulated phosphoinositide hydrolysis in HeLa cells is well characterised (Tilly *et al.*, 1990b; Bristow *et al.*, 1991) and we have provided evidence that the binding properties of the H_1-receptor mediating the response are similar to those of H_1-receptors in mammalian brain (Arias-Montaño & Young, 1993a). The dependence of phosphoinositidase C (PIC) on low levels of intracellular Ca^{2+} has also been demonstrated in these cells (Tilly *et al.*, 1990a). However, it has been suggested that in non-excitable cells, such as epithelia, Ca^{2+} entry mechanisms may be confined to that associated with the refilling of 1,4,5-IP_3-sensitive intracellular stores (Putney, 1990). The lack in HeLa cells, a line derived from human uterine cervical epithelium, of any effect on histamine-induced [^{3}H]-IP_1 formation of increasing the extracellular Ca^{2+} above 0.3 mM would be consistent with this proposition. It also suggests that HeLa cells may be valuable as a model system on which to study H_1-receptor/G protein activation of PIC without the complication of an additional component in the mechanism dependent on extracellular Ca^{2+}. The presence of a response to carbachol in HeLa cells gives the added advantage of a second receptor system coupled to PIC, which can in principle be used as a control for H_1-receptor-specific effects of agents or treatments. It is probable that the muscarinic receptor mediating the response to carbachol is of the M_3-subtype, as in U373 MG cells, but the lack of strict parallelism in the concentration-response curves in the presence and absence of pirenzepine indicates the need for a more detailed study. In U373 MG cells the evidence from the K_d for pirenzepine for the involvement of M_3-muscarinic receptors in carbachol-stimulated [^{3}H]-IP_1 accumulation is given some indirect support by the report of M_3-receptor mediation of [^{3}H]-IP_1 formation in 1321N human astrocytoma cells (Kunysz *et al.*, 1989). In rat cerebral cortex the response to muscarinic agonists appears to be mediated predominantly by M_1-receptors (Forray & El-Fakahany, 1990).

The pattern of the Ca^{2+}-dependence of carbachol stimulated [^{3}H]-IP_1 accumulation is similar in HeLa cells, U373 MG cells, and guinea-pig and rat brain slices. This is not the case with histamine-induced [^{3}H]-IP_1 accumulation. Not only does the pattern differ between U373 MG and HeLa cells, there is also a clear species difference between rat and guinea-pig cerebral cortex, which is also evident in the data of Alexander *et al.* (1990b) over a more limited range of Ca^{2+} concentrations. The difference between guinea-pig cerebral cortex and cerebellum lies largely in the magnitude of the initial increase between no added Ca^{2+} and 0.3 mM Ca^{2+}, which could reflect the difference in H_1-receptor density between the two tissues (Hill *et al.*, 1978). Whether any of the difference in the pattern between rat cerebral cortex (Figure 8a), in which there is indirect evidence for location of at least some H_1-receptors on astrocytes (Arbonés *et al.*, 1990), and guinea-pig cerebellum (Figure 8c), where the receptors may be neuronal (Palacios *et al.*, 1981), reflects a differing cellular locus is unknown. However, it is clear that not all brain tissues show the same very marked dependence on extracellular Ca^{2+} as mouse and rat cerebral cortex and the Ca^{2+}-dependence observed in the U373 MG cells is much closer to that in the guinea-pig tissues. There is as yet no indication whether this is also the pattern in human cerebral cortex, a tissue in which histamine is known to stimulate phosphoinositide hydrolysis (Kendall & Firth, 1990) and it would be unwise to make predictions on the basis of the response in a transformed cell line.

The difference between histamine and carbachol in the pattern of Ca^{2+}-dependence of [^{3}H]-IP_1 accumulation in U373 MG cells is lessened by the increase in the response to carbachol between 0.3 and 1.3 mM Ca^{2+} (Figure 6a). However, the difference is clearer in the comparisons of the Ca^{2+}-dependence of [^{3}H]-IP_2 and [^{3}H]-IP_3 formation (Figure 5b,c; Figure 6b,c), although the amount of material in the trisphosphate fraction in the presence of carbachol is small. The modest decline in the [^{3}H]-IP_1 response to carbachol between 1.3 and 4 mM Ca^{2+} in U373 MG cells could conceivably reflect the reported inhibition of the response to carbachol by Ca^{2+} (Baird *et al.*, 1989), although this effect is not otherwise apparent in our measurements.

A better understanding of the significance of the modest Ca^{2+}-dependence of the histamine-response in U373 MG cells will become clearer when selective blockade of the Ca^{2+}-dependent component in brain tissue becomes possible. Neither L-type nor N-type Ca^{2+} channels appear to be involved and the use of divalent cations such as Ni^{2+} as non-selective blockers of Ca^{2+} entry is complicated by a possible additional action at the level of the H_1-receptor, evident in the inhibition by Cd^{2+}, Zn^{2+}, Ni^{2+} and Co^{2+} of [^{3}H]-mepyramine binding to guinea-pig cerebellar membranes (Treherne *et al.*, 1991). The secondary action of Ni^{2+} on histamine-induced [^{3}H]-IP_1 formation, without affecting the response to carbachol, has been demonstrated directly in HeLa cells, illustrating their utility as a model system (Arias-Montaño & Young, 1993b). The availability of a selective blocker for the presumed Ca^{2+}-entry component in brain slices would provide a much simpler and more satisfactory assay than the measurement of Ca^{2+}-dependence for screening cell lines as possible model systems. It would also enable an approach to be made to the central question of the functional significance of the Ca^{2+}-dependent component at the normal Ca^{2+} concentration, *circa* 1.3 mM, of the cerebrospinal fluid.

We are grateful to the Wellcome Trust for financial support and to Martin Bootman for kindly providing the S3 HeLa cell clone.

References

ALEXANDER, S.P.H., HILL, S.J. & KENDALL, D.A. (1990a). Differential effects of elevated calcium ion concentrations on inositol phospholipid responses in mouse and rat cerebral cortical slices. *Biochem. Pharmacol.*, **40**, 1793–1799.

ALEXANDER, S.P.H., HILL, S.J. & KENDALL, D.A. (1990b). Is the adenosine receptor modulation of histamine-induced accumulation of inositol phosphates in cerebral cortical slices mediated by effects on calcium ion fluxes? *J. Neurochem.*, **55**, 1138–1141.

ARBONÉS, L., PICATOSTE, F. & GARCIA, A. (1988). Histamine H_1-receptors mediate phosphoinositide hydrolysis in astrocyte-enriched primary cultures. *Brain Res.*, **450**, 144–152.

ARBONÉS, L., PICATOSTE, F. & GARCIA, A. (1990). Histamine stimulates glycogen breakdown and increases $^{45}Ca^{2+}$ permeability in rat astrocytes in primary culture. *Mol. Pharmacol.*, **37**, 921–927.

ARIAS-MONTAÑO, J.A. & YOUNG, J.M. (1992). Different patterns of Ca^{2+}-dependence of histamine-induced inositol phosphate formation in HeLa cells and rat brain. *Br. J. Pharmacol.*, **105**, 23P.

ARIAS-MONTAÑO, J.A. & YOUNG, J.M. (1993a). Characteristics of histamine H_1 receptors on HeLa cells. *Eur. J. Pharmacol.*, **245**, 291–295.

ARIAS-MONTAÑO, J.A. & YOUNG, J.M. (1993b). Locus of action of Ni^{2+} on histamine-induced inositol phosphate formation in brain slices and in HeLa cells. *Eur. J. Pharmacol.*, **245**, 221–228.

BAIRD, J.G., CHILVERS, E.R., KENNEDY, E.D. & NAHORSKI, S.R. (1989). Changes in extracellular calcium within the physiological range influence receptor-mediated inositol phosphate responses in brain and tracheal smooth muscle slices. *Naunyn-Schmied Arch. Pharmacol.*, **339**, 247–251.

BAIRD, J.G. & NAHORSKI, S.R. (1990). Increased intracellular calcium stimulates ^{3}H-inositol polyphosphate accumulation in rat cerebral cortical slices. *J. Neurochem.*, **54**, 555–561.

BRISTOW, D.R., ARIAS-MONTAÑO, J.A. & YOUNG, J.M. (1991). Histamine-induced inositol phosphate accumulation in HeLa cells: lithium sensitivity. *Br. J. Pharmacol.*, **104**, 677–684.

CHANG, R.S.L., TRAN, V.T. & SNYDER, S.H. (1980). Neurotransmitter receptor localizations: brain lesion induced alterations in benzodiazepine, GABA, β-adrenergic and histamine H_1-receptor binding. *Brain Res.*, **190**, 95–110.

CULVENOR, A.J. & JARROTT, B. (1981). Comparison of histamine H_1-receptors in bovine intracerebral microvessels with cerebral grey matter by [^{3}H]mepyramine binding. *Neurochem. Int.*, **3**, 365–369.

DAUM, P.R., DOWNES, C.P. & YOUNG, J.M. (1983). Histamine-induced inositol phospholipid breakdown mirrors H_1-receptor density in brain. *Eur. J. Pharmacol.*, **87**, 497–498.

DOWNES, C.P., HAWKINS, P.T. & IRVINE, R.F. (1986). Inositol 1,3,4,5-tetrakisphosphate and not phosphatidylinositol 3,4-bisphosphate is the probable precursor of inositol 1,3,4-trisphosphate in agonist-stimulated parotid gland. *Biochem. J.*, **238**, 501–506.

EBERHARD, D.A. & HOLZ, R.W. (1988). Intracellular Ca^{2+} activates phospholipase C. *Trends Neurosci.*, **11**, 517–520.

FORRAY, C. & EL-FAKAHANY, E.E. (1990). On the involvement of multiple muscarinic receptor subtypes in the activation of phosphoinositide metabolism in rat cerebral cortex. *Mol. Pharmacol.*, **37**, 893–902.

GOH, Y. & KUROSAWA, A. (1991). Characterization and Ca^{2+} requirement of histamine-induced catecholamine secretion in cultured bovine chromaffin cells. *J. Neurochem.*, **57**, 1249–1257.

HILL, S.J. (1990). Distribution, properties and functional characteristics of three classes of histamine receptor. *Pharmacol. Rev.*, **42**, 45–82.

HILL, S.J., EMSON, P.C. & YOUNG, J.M. (1978). The binding of [^{3}H]mepyramine to histamine H_1 receptors in guinea-pig brain. *J. Neurochem.*, **31**, 997–1004.

HULME, E.C., BIRDSALL, N.J.M. & BUCKLEY, N.J. (1990). Muscarinic receptor subtypes. *Annu. Rev. Pharmacol. Toxicol.*, **30**, 633–673.

INAGAKI, N., FUKUI, H,. TAGUCHI, Y., WANG, N.P., YAMOTADANI, A. & WADA, H. (1989). Characterization of histamine H_1-receptors on astrocytes in primary culture: [^{3}H]-mepyramine binding studies. *Eur. J. Pharmacol.*, **173**, 43–51.

INAGAKI, N., FUKUI, H., ITO, S., YAMOTADANI, A. & WADA, H. (1991). Single type-2 astrocytes show multiple independent sites of Ca^{2+} signaling in response to histamine. *Proc. Natl. Acad. Sci. U.S.A.*, **88**, 4215–4219.

JOHNSON, C.L. & JOHNSON, C.G. (1992). Characterization of receptors for substance P in human astrocytoma cells: radioligand binding and inositol phosphate formation. *J. Neurochem.*, **58**, 471–477.

KENDALL, D.A. & FIRTH, J.L. (1990). Inositol phospholipid hydrolysis in human brain; adenosine inhibition of the response to histamine. *Br. J. Pharmacol.*, **100**, 37–40.

KENDALL, D.A. & NAHORSKI, S.R. (1984). Inositol phospholipid hydrolysis in rat cerebral cortical slices: II. Calcium requirement. *J. Neurochem.*, **42**, 1388–1394.

KNEPPER, S.M. & RUTLEDGE, C.O. (1987). Effects of calcium depletion on norepinephrine- and A23187-induced stimulation of inositol phosphate formation. *Biochem. Pharmacol.*, **36**, 3043–3050.

KOMORI, S., KAWAI, M., TAKEWAKI, T. & OHASHI, H. (1992). GTP-binding protein involvement in membrane currents evoked by carbachol and histamine in guinea-pig ileal muscle. *J. Physiol.*, **450**, 105–126.

KONDOU, H., INAGAKI, N., FUKUI, H., KOYAMA, Y., KANAMURA, A. & WADA, H. (1991). Histamine-induced inositol phosphate accumulation in type-2 astrocytes. *Biochem. Biophys. Res. Commun.*, **177**, 734–738.

KUNYSZ, E.A., MICHEL, A.D., WHITING, R.L. & WOODS, K. (1989). The human astrocytoma cell line 1321N1 contains M_2-glandular type muscarinic receptors linked to phosphoinositide turnover. *Br. J. Pharmacol.*, **96**, 271–278.

LOWRY, O.H., ROSEBROUGH, N.J., FARR, A.L. & RANDALL, R.J. (1951). Protein measurements with the Folin phenol reagent. *J. Biol. Chem.*, **193**, 265–275.

LUCHERINI, M.J. & GRUENSTEIN, E. (1992). Histamine H_1 receptors in UC-11MG astrocytes and their regulation of cytoplasmic Ca^{2+}. *Brain Res.*, **592**, 193–201.

MEDRANO, S., GRUENSTEIN, E. & DIMLICH, R.V.W. (1992). Histamine stimulates glycogenolysis in human astrocytoma cells by increasing intracellular free calcium. *Brain Res.*, **592**, 202–207.

MICHEL, M.C., HANFT, G. & GROSS, G. (1990). α_{1B}- but not α_{1A}-adrenoceptors mediate inositol phosphate generation. *Naunyn-Schmied. Arch. Pharmacol.*, **341**, 385–387.

MINNEMAN, K.P. & ATKINSON, B. (1991). Interaction of subtype-selective antagonists with α_1-adrenergic receptor-mediated second messenger responses in rat brain. *Mol. Pharmacol.*, **40**, 523–530.

MURPHY, S. & PEARCE, B. (1987). Functional receptors for neurotransmitters on astroglial cells. *Neurosci.*, **22**, 381–394.

NAKAHATA, N., MARTIN, M.W., HUGHES, A.R., HEPLER, J.R. & HARDEN, T.K. (1986). H_1-Histamine receptors on human astrocytoma cells. *Mol. Pharmacol.*, **29**, 188–195.

PALACIOS, J.M., WAMSLEY, J.K. & KUHAR, M.J. (1981). GABA, benzodiazepine and histamine-H_1 receptors in the guinea pig cerebellum: effects of kainic acid injections studied by autoradiographic methods. *Brain Res.*, **214**, 155–162.

PEROUTKA, S.J., MOSKOWITZ, M.A., RIENHARD, Jr, J.F. & SNYDER, S.H. (1980). Neurotransmitter receptor binding in bovine cerebral microvessels. *Science*, **208**, 610–612.

PUTNEY, Jr, J.W. (1990). Capacitative calcium reentry revisited. *Cell Calcium*, **11**, 611–624.

QUACH, T.T., DUCHEMIN, A.-M., ROSE, C. & SCHWARTZ, J.-C. (1980). ^{3}H-Glycogen hydrolysis elicited by histamine in mouse brain slices: selective involvement of H_1 receptors. *Mol. Pharmacol.*, **17**, 301–308.

RODBARD, D. (1974). Statistical quality control and routine data processing for radioimmunoassays and immunoradiometric assays. *Clin. Chem.*, **20**, 1255–1270.

SCHWARTZ, J.-C., ARRANG, J.-M., GARBARG, M., POLLARD, H. & RUAT, M. (1991). Histaminergic transmission in mammalian brain. *Physiol. Rev.*, **71**, 1–51.

SHARPES, E.S. & MCCARL, R.L. (1982). A high-performance liquid chromatographic method to measure ^{32}P incorporation into phosphorylated metabolites in cultured cells. *Anal. Biochem.*, **124**, 421–424.

SUMMERS, R.J. & MCMARTIN, L.R. (1993). Adrenoceptors and their second messenger systems. *J. Neurochem.*, **60**, 10–23.

TILLY, B.C., LAMBRECHTS, A.C., TERTOOLEN, L.G.J., DE LAAT, S.W. & MOOLENAAR, W.H. (1990a). Regulation of phosphoinositide hydrolysis induced by histamine and guanine nucleotides in human HeLa carcinoma cells. *FEBS Lett*, **265**, 80–84.

TILLY, B.C., TERTOOLEN, L.G.J., LAMBRECHTS, A.C., REMORIE, R., DE LAAT, S.W. & MOOLENAAR, W.H. (1990b). Histamine-H_1-receptor-mediated phosphoinositide hydrolysis, Ca^{2+} signalling and membrane-potential oscillations in human HeLa carcinoma cells. *Biochem. J.*, **266**, 235–243.

TREHERNE, J.M., STERN, J.S., FLACK, W.J. & YOUNG, J.M. (1991). Inhibition by cations of antagonist binding to histamine H_1-receptors: differential effect of sodium ions on the binding of two radioligands. *Br. J. Pharmacol.*, **103**, 1745–1751.

WEISS, S., SCHMIDT, B.H., SEBBEN, M., KEMP, D., BOCKAERT, J. & SLADECZEK, F. (1988). Neurotransmitter-induced inositol phosphate formation in neurons in primary culture. *J. Neurochem.*, **50**, 1425–1433.

YAMAMOTO, Y., CHEN, G., MIWA, K. & SUZUKI, H. (1992). Permeability and Mg^{2+}-blockade of histamine-operated cation channel in endothelial cells of rat intrapulmonary artery. *J. Physiol.*, **450**, 395–408.

(Received September 1, 1993
Revised October 15, 1993
Accepted October 18, 1993)